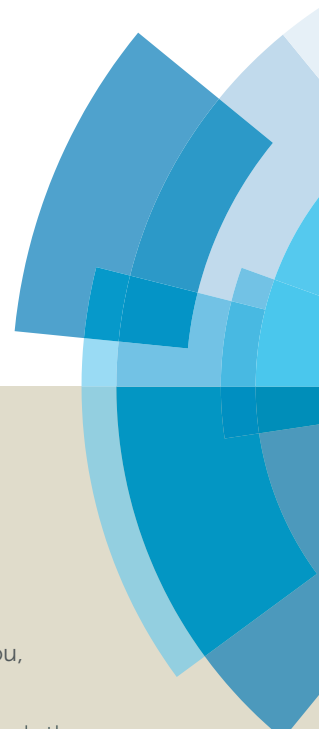
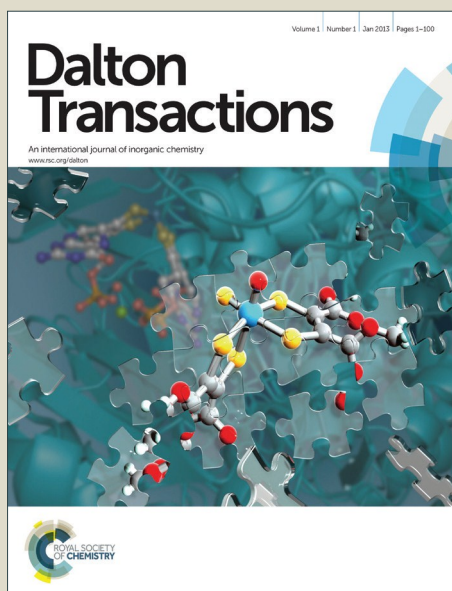


Dalton Transactions

Accepted Manuscript



This article can be cited before page numbers have been issued, to do this please use: G. Chen, W. Hou, J. Li, X. Wang, Y. Zhou and J. Wang, *Dalton Trans.*, 2016, DOI: 10.1039/C6DT00070C.



This is an *Accepted Manuscript*, which has been through the Royal Society of Chemistry peer review process and has been accepted for publication.

Accepted Manuscripts are published online shortly after acceptance, before technical editing, formatting and proof reading. Using this free service, authors can make their results available to the community, in citable form, before we publish the edited article. We will replace this *Accepted Manuscript* with the edited and formatted *Advance Article* as soon as it is available.

You can find more information about *Accepted Manuscripts* in the [Information for Authors](#).

Please note that technical editing may introduce minor changes to the text and/or graphics, which may alter content. The journal's standard [Terms & Conditions](#) and the [Ethical guidelines](#) still apply. In no event shall the Royal Society of Chemistry be held responsible for any errors or omissions in this *Accepted Manuscript* or any consequences arising from the use of any information it contains.

Journal Name

COMMUNICATION

Ionic self-assembly affords mesoporous ionic networks by crosslinking linear polyviologens with polyoxometalate clusters

Guojian Chen,^{a,b} Wei Hou,^a Jing Li,^a Xiaochen Wang,^a Yu Zhou*^a and Jun Wang*^aReceived 00th January 20xx,
Accepted 00th January 20xx

DOI: 10.1039/x0xx00000x

www.rsc.org/

Ionic-bonded mesoporous ionic networks were prepared by the ionic self-assembly of polyoxometalate (POM) clusters with linear cationic polyviologens in water. The POM-enriched PMIN-1(V) possesses a high surface area up to 120 m² g⁻¹, exhibiting superior non-noble metal heterogeneous catalytic performance in the ambient aerobic selective oxidation of 5-hydroxymethylfurfural.

Functional porous materials have received ever-increasing attention because of their wide applications in adsorption, separation, catalysis, energy storage, electrode materials, etc.^{1–11} Self-assembly method enables the facilely and elegantly fabrication of numerous versatile porous materials from diverse molecular building blocks, and has become a hot topic in chemical and materials science. Different driving forces afford different series of porous materials. For instance, it is feasible to self-assembly synthesis of metal-organic frameworks (MOFs) by coordination bonds,² crystalline covalent organic frameworks (COFs) and amorphous porous organic polymers (POPs) by covalent bonds,^{3,4} and hydrogen-bonded organic frameworks (HOFs) via weaker hydrogen-bonding interactions.^{5,6} Nonetheless, as a large class of widely applied materials, ionic bonded inorganic or inorganic/organic hybrid salts are scarcely prepared to possess large open porous networks. To the best of our knowledge, no such type porous ionic-bonded frameworks attains through ionic bond derived self-assembly method, i.e. the ionic self-assembly (ISA) approach,¹² despite that ISA achieves various success as a powerful tool to afford hierarchical nanostructured materials by the electrostatic coupling of carefully chosen charged surfactants or polymers and oppositely charged building blocks.^{12,13}

Polyoxometalates (POM) are an outstanding family of structurally diverse anionic metal-oxo clusters with tunable engaging physical and chemical properties by structure designation from the

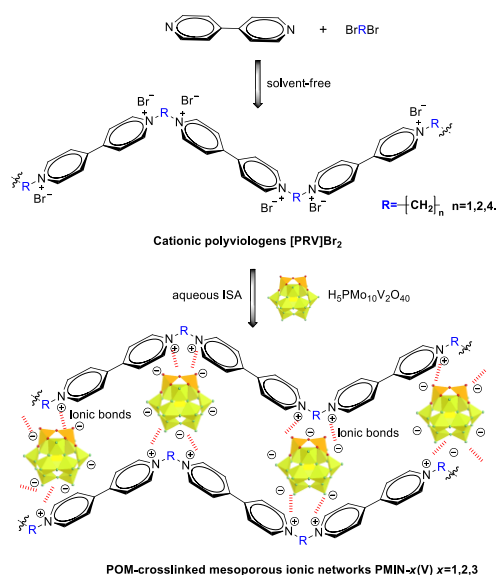
molecular or atomic level to the nano and even to the micrometer scale.¹⁴ They have been widely used as nanoscale building blocks for constructing various supermolecular materials, enabling the facile preparation of uniform self-supported functional materials with high POM density towards a large domains of applications.^{14,15} Both order and disorder POM based supermolecular assemblies were reported by self-assembly approach,¹⁶ but majority of them were nonporous structure or possessed low surface area,^{17–20} limiting their performance in the processes involving mass transfer step such as catalysis, one main application of POMs.

In this work, we try to apply ISA strategy towards self-assembled porous ionic networks by the cooperative combination of linear cationic polymers and multivalent anionic building blocks. A series of novel POM-based mesoporous ionic networks (shorten as PMINs) are constructed by crosslinking linear cationic polyviologens with POM anionic clusters via ionic-bonding interactions. Polyviologens containing 1,1'-dialkyl-4,4'-bipyridinium repeated units are a well-known class of cationic polymers with photoelectrochromism, electron-accepting ability and redox activity.^{21,22} This tactic could *in-situ* incorporate catalytically active POM building blocks and redox viologen units into the resulted PMINs, simultaneously reaching organic-inorganic hybrid mesoporous ionic nanostructures with unprecedented high surface areas (120 m² g⁻¹) and available redox catalytic properties. Thus, the typical PMoV-enriched PMINs act as highly efficient heterogeneous catalysts in the ambient selective aerobic oxidation of 5-hydroxymethylfurfural into 2,5-diformylfuran with molecular oxygen (O₂).

Scheme 1 illustrates the synthetic process for PMoV-based mesoporous ionic networks PMIN-x(V) by using different polyviologens [PMV]Br₂, [PEV]Br₂ and [PBV]Br₂ for x=1, 2 and 3 respectively. Three new alkyl-linked polyviologens are prepared by the quaternization reaction of 4,4'-bipyridine with dibromoalkane.²¹ The resulted water-soluble linear polymers polyviologens have repeat cationic units of 4,4'-bipyridinium with alkyl linkers, as confirmed by ¹H NMR, ¹³C NMR, FT-IR spectra and elemental analysis (Figs. S1–S3 and S6). The molecular weights (M_w) of [PMV]Br₂, [PEV]Br₂ and [PBV]Br₂ are 19948, 19810 and 19694 Da, respectively (Fig. S7). Electrostatic interactions induced ionic self-assembly between the above three polyviologens and PMoV anions

^a State Key Laboratory of Materials-Oriented Chemical Engineering, College of Chemical Engineering, Nanjing Tech University, Nanjing, 210009, China. E-mail: njtuzhouyu@njtech.edu.cn, junwang@njtech.edu.cn; Tel: +(86) 25-83172264. ^b School of Chemistry and Chemical Engineering, Jiangsu Normal University, Xuzhou, 221116, China.

† Footnotes relating to the title and/or authors should appear here. Electronic Supplementary Information (ESI) available: [Experimental section, Figures S1–S16, Tables S1–S3 and Scheme S1]. See DOI: 10.1039/x0xx00000x.



Scheme 1 Synthetic process for constructing PMINs from ionic self-assembly of cationic polyviologens and PMoV in aqueous solution.

in aqueous solution affords three PMIN-*x*(V) samples. Elemental analysis results in Table S1 provide specific molecular formulas and chemical compositions for each PMIN sample.

Scanning electron microscopy (SEM) images (Fig. 1A-C and Fig. S8) reveal that PMIN-*x*(V) have sponge-like mesoporous structures derived from the packing of interconnected nanoparticles with the sizes of about 20-30 nm. PMIN-1(V) has the most loosely-packed secondary nanostructures, and PMIN-2(V) exhibits moderate spatial arrangement, while PMIN-3(V) demonstrates closely-packed array. Mesopores come from the nano-voids among these aggregated nanoparticles for constructing the crosslinked ionic networks, which are further confirmed by the results of TEM images (Fig. 1D-F). The quantitative analysis of the pore structure of above PMIN-*x*(V) samples is measured by N₂ sorption experiments. Fig. 2 shows that all the adsorption isotherms are type IV with a clear H1-type hysteresis loop at the relative pressure (P/P_0) range from 0.5 to 0.9, indicative of typical mesoporous materials. Barrett-Joyner-Halenda (BJH) pore size distributions of PMIN-*x*(V) exhibit a very narrow mesopore size distribution centred at 9.2 nm for PMIN-2(V), small mesopore size around 4 nm for PMIN-3(V), and a wide mesopore size distribution ranging from several to more than ten nm for PMIN-1(V). The described mesopore sizes of PMIN-*x*(V) are closely consistent with the compactness of interconnected particles, as observed by the SEM and TEM images (Fig. 1A-1F).

Table 1 list textural parameters including the Brunauer-Emmett-Teller surface areas (S_{BET}), pore volume (V_p) and average pore sizes (D_{av}). The results indicate that PMIN-*x*(V) have very high BET surface areas ranging from 72 m² g⁻¹ to 120 m² g⁻¹, with the large pore volume of 0.17-0.28 cm³ g⁻¹. PMIN-2(V) gives the highest surface area of 120 m² g⁻¹, superior to those values (25-51 m² g⁻¹) of all the reported porous POM hybrids paired with organic or metal-organic cations (e.g. triammonium cations,²³ ionic liquids,^{24,25} cationic transition-metal complexes and zinc phosphate^{26,27}), even surpass poly(ionic liquid)-supported POMs,^{28,29} and comparable to the surface areas (85-156 m² g⁻¹) for the conventional micro-/mesoporous NH₄⁺ and Cs⁺ salts of POMs.³⁰ Details comparison is

summarized in Table S2. Noticeably, those inorganic cations modified POMs were usually of microporous structures with small amount of mesopore. It is the first time to achieve such abundant mesopores over self-assembled POMs, endowing high POM anions density on the surface of a homogeneous framework.

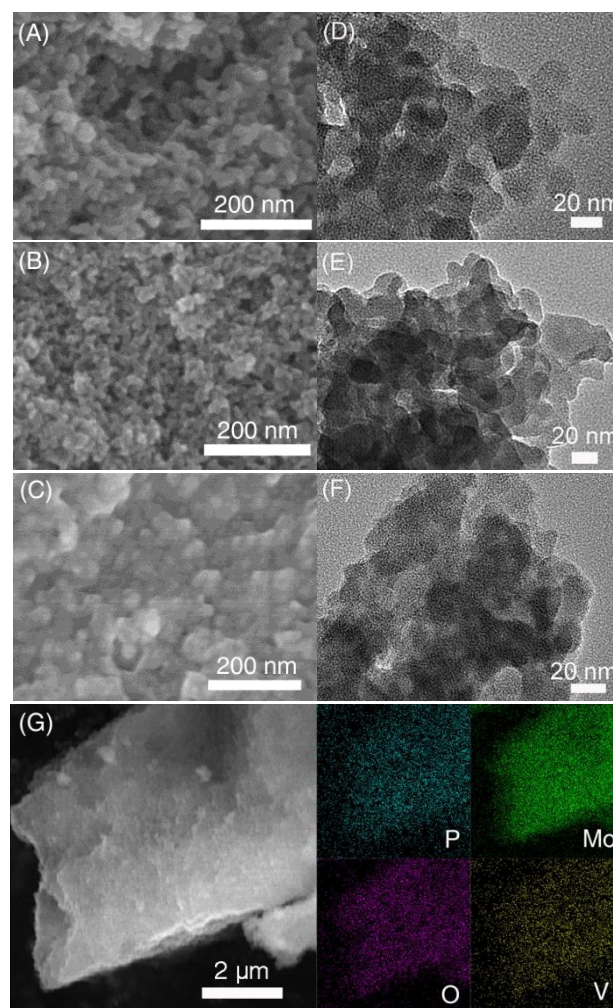


Fig. 1 SEM images of (A) PMIN-1(V), (B) PMIN-2(V) and (C) PMIN-3(V). TEM images of (D) PMIN-1(V), (E) PMIN-2(V) and (F) PMIN-3(V). (G) Energy-dispersive X-ray spectrometry (EDS) elemental mapping analysis of the sample PMIN-2(V).

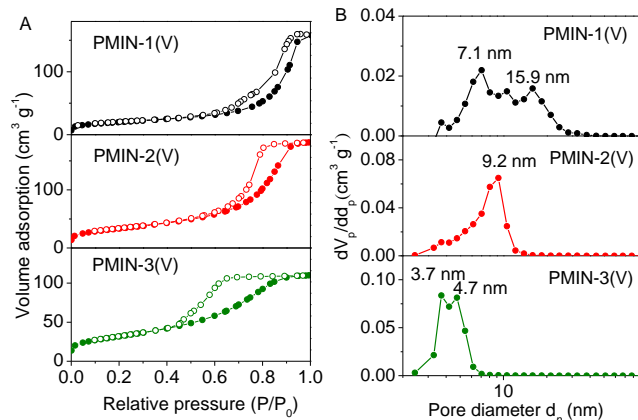


Fig. 2 (A) N₂ sorption isotherms and (B) Pore size distributions of PMIN-*x*(V) samples calculated by BJH method.

Table 1 The textural parameters of PMIN-x(V) series materials.

PMINs	S_{BET} ($\text{m}^2 \text{g}^{-1}$) ^a	V_p ($\text{cm}^3 \text{g}^{-1}$) ^b	D_{av} (nm) ^c
PMIN-1(V)	72	0.24	13.42
PMIN-2(V)	120	0.28	9.33
PMIN-3(V)	115	0.17	5.90

^a BET surface area. ^b Pore volume. ^c Average pore sizes.

Besides, another two common POM anions $\text{PMo}_{12}\text{O}_{40}^{3-}$ (PMo) and $\text{PW}_{12}\text{O}_{40}^{3-}$ (PW) are employed as anionic cross-linkers to fabricate porous ionic networks. Taking $[\text{PMV}]\text{Br}_2$ as the linear cationic polymer, the produced PMIN-1(Mo) and PMIN-1(W) also demonstrate mesoporous structure with narrow mesopore size distributions (Fig. S9 and S10). The surface areas for them are 60 and $26 \text{ m}^2 \text{g}^{-1}$, inferior to the one over PMIN-1(V). The above phenomena suggest that different mesoporous structure can be achieved by varying the cations and anions.

Thermogravimetric (TG) analyses (Fig. S11) of PMIN-x(V) illustrate their structure stable up to 250°C . The total weight loss reflects the high content (71-73 wt %) of PMoV anions within the networks of PMIN-x(V), close to their theoretical values according to their molecular formulas obtained from elemental analysis results (Table S1). PMoV anions in mesoporous ionic networks are investigated by spectral characterizations (Fig. 3). In Fig. 3A, FT-IR spectra of PMIN-x(V) show the presence of Keggin-type PMoV cluster by featured peaks at 1071 and 1053 cm^{-1} $\nu(\text{P-O}_a)$, 945 cm^{-1} $\nu(\text{M-O}_b\text{-M})$ ($\text{M}=\text{Mo}$ or V), 872 cm^{-1} $\nu(\text{M-O}_c\text{-M})$ and 785 cm^{-1} $\nu(\text{M-O}_d)$ with slight shifts compared with parent $\text{H}_5\text{PMo}_{10}\text{V}_2\text{O}_{40}$.²⁸ A new broad Bragg peak in the XRD patterns (Fig. 3B) of PMIN-x(V) appears at $2\theta=8.27\text{-}8.65^\circ$ with the d -spacing values of $1.02\text{-}1.07 \text{ nm}$, very close to the primary unit of PMoV anion. This result indicates that certain ordered mesostructure forms during the self-assembly process, and PMoV clusters (*ca.* 1.0 nm) are homogeneously well-dispersed in the ionic network, which is further demonstrated by the EDS elemental mapping analysis for P, O, Mo, V elements (Fig. 1G) and XPS survey spectrum (Fig. 3E). The electronic behaviours of PMoV-incorporated PMIN-x(V) are examined by UV-vis, ESR and XPS spectra. The UV-vis spectra (Fig. 3C) of PMIN-x(V) show apparent enhanced adsorption bands at $600\text{-}800 \text{ nm}$ with respect to parent $\text{H}_5\text{PMo}_{10}\text{V}_2\text{O}_{40}$, which is assigned to the reduced state of V^{4+} species. The coexistence of $\text{V}^{5+}/\text{V}^{4+}$ species is further confirmed by the typical eight fold hyperfine splitting signals centred at $G=3500$ in ESR spectra (Fig. 3D),¹⁰ while the ESR signals for $\text{H}_5\text{PMo}_{10}\text{V}_2\text{O}_{40}$ are silent. Moreover, the XPS V2p spectrum confirms the electronic-state of V species, *i.e.* the two peaks appeared at 524.3 and 517.0 eV are assigned to $\text{V}2p_{1/2}$ and $\text{V}2p_{3/2}$, and the adjunctive two peaks appeared at 525.9 and 515.4 eV corresponds to $\text{V}2p_{1/2}$ and $\text{V}2p_{3/2}$, indicating the present of V^{5+} and V^{4+} species, respectively.¹⁰ Based on the above results, π -conjugated redox cationic polyviologens can dramatically affect the charge state of PMoV anions, promoting the formation of V^{4+} species-rich PMIN-x(V), which is beneficial to catalyse many oxidative reactions.

The large surface areas, nanoscale morphologies and high PMoV contents of mesoporous ionic networks PMIN-x(V) encourage us to employ them as heterogeneous catalysts in the O_2 -mediated oxidation of biomass-derived 5-hydroxymethylfurfural (HMF) to 2,5-diformylfuran (DFF), a very important precursor or monomer for

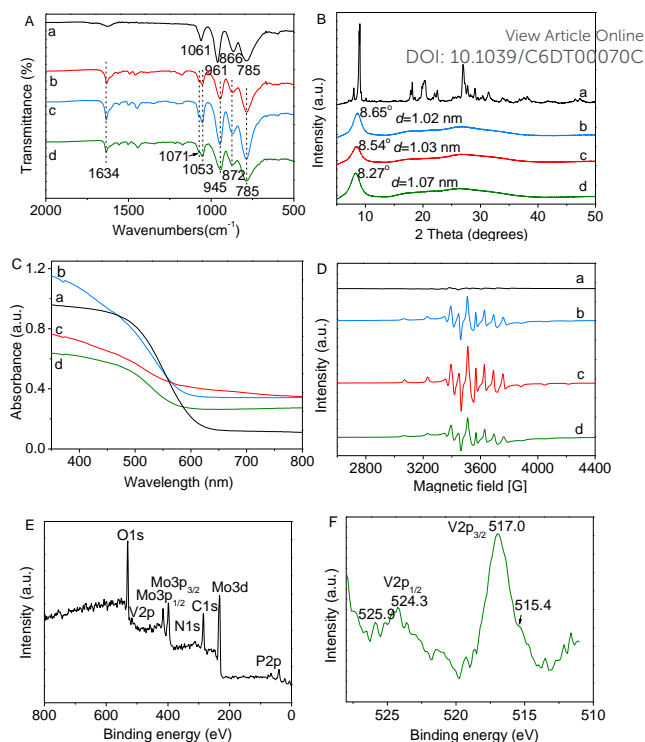
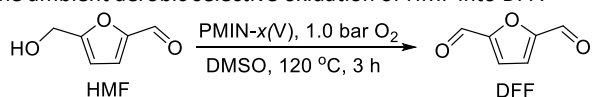


Fig. 3 (A) XRD patterns, (B) FT-IR spectra, (C) UV-vis spectra and (D) ESR spectra of (a) $\text{H}_5\text{PMo}_{10}\text{V}_2\text{O}_{40}$, (b) PMIN-1(V), (c) PMIN-2(V) and (d) PMIN-3(V). (E) XPS survey and (F) V2p spectrum of PMIN-2(V).

producing high value-added fine chemicals and functional polymers.³¹ Table 2 lists the catalytic performances PMIN-x(V) and their counterparts in the conversion of HMF to DFF under ambient O_2 condition. It is noteworthy that POM $\text{H}_5\text{PMo}_{10}\text{V}_2\text{O}_{40}$ is discovered to be efficient in transforming HMF into DFF, affording a high HMF conversion of 97.0% and moderate DFF yield of 80.4% under optimized conditions (Fig. S12). Owing to its soluble in the reaction solution, $\text{H}_5\text{PMo}_{10}\text{V}_2\text{O}_{40}$ results a homogeneous catalytic system. By contrast, all PMIN-x(V) samples resist the dissolution even in DMSO, thus perform remarkably heterogeneous catalytic activities with DFF yields of 71.4-86.8%. Among them, PMIN-2(V) gives the highest HMF conversion of 100%, DFF yield of 86.8%, and turnover number (TON) of 121. Such catalytic activity is superior to the homogeneous $\text{H}_5\text{PMo}_{10}\text{V}_2\text{O}_{40}$, much higher than many vanadium-based catalysts,³²⁻³⁴ and even comparable to noble metal (*e.g.* Ru) catalysts^{35,36} under ambient condition (see Table S3). Importantly, in a five-run recycling test (Fig. S13), PMIN-2(V) can be directly reused after facile separation by filtration and maintains initial high activities as the fresh one, exhibiting well stable reusability. Full characterizations (FT-IR, N_2 sorption and SEM, see Figs. S14-S16) of the recovered PMIN-2(V) demonstrate the preservation of chemical composition and porous structure, accounting for its well recycling performance.

For comparison, parallel tests are carried out on the non-polymeric viologen-POM ionic hybrid catalysts $[\text{Bpy}]_{2.5}\text{PMoV}_2$, $[\text{C}_2\text{Bpy}]_{2.5}\text{PMoV}_2$ and $[\text{C}_4\text{Bpy}]_{2.5}\text{PMoV}_2$ with similar chemical compositions as the repeating unit of PMIN-x(V) (see ESI). Surprisingly, all of them fail to cause heterogeneous systems and present inferior activities with HMF conversions of 43.6-76.8% and DFF yields of 39.9-76.6% (Table 2). The above results indicate the

Table 2 Catalytic performance of PMIN-x(V) and their counterparts in the ambient aerobic selective oxidation of HMF into DFF.^a



Catalyst	Reaction system	HMF C (%) ^b	DFF S (%) ^c	DFF Y (%) ^d	TON ^e
H ₅ PMo ₁₀ V ₂ O ₄₀	Homo.	97.0	82.9	80.4	112
PMIN-1(V)	Heter.	80.0	89.2	71.4	99
PMIN-2(V)	Heter.	100	86.8	86.8	121
PMIN-3(V)	Heter.	97.5	82.9	80.8	112
[Bpy] _{2.5} PMoV ₂	Homo.	76.8	99.7	76.6	106
[C ₂ Bpy] _{2.5} PMoV ₂	Homo.	74.6	81.7	60.9	85
[C ₄ Bpy] _{2.5} PMoV ₂	Homo.	43.6	91.5	39.9	55

^a Reaction conditions: HMF (100.8 mg, 0.80 mmol), catalyst (0.01 g, 5.76 μmol based on PMoV), oxygen balloon 1.0 bar, DMSO 4 mL, 120 °C, 3 h. ^b Conversion (C) of HMF. ^c Selectivity (S) of DFF. ^d Yield (Y) of DFF. ^e Turnover number (TON): mole of product DFF per mol of PMoV in the catalyst.

designed alkyl-linked cationic polyviologens play the vital role towards efficient mesoporous POM-based heterogeneous catalysts for HMF conversion. Polycations enable the heterogeneous property of PMoV anions through providing strong and complex interaction between multivalent cations and anions. On the contrary, dications are incapable to fabricate solid POM catalyst facing with DMSO as solvent due to the strong solubility of POM in DMSO, though various dication modified POM solid catalysts have been achieved by using other solvents. The high catalytic activity, especially for PMIN-2(V), can be attributed to that large surface area and abundant mesoporosity allows the well dispersion of V-O-V (V⁵⁺/V⁴⁺) catalytically active species and suitable accommodation for the substrates and products. The proposed catalytic mechanism for aerobic oxidation of HMF to DFF is presented in Scheme S1 with the detailed explanation. Owing to the improved mass transfer and high density of active sites, only small amount of PMIN-x(V) is able to efficiently convert HMF to DFF, differing from previous reported catalytic systems for this reaction. Correspondingly, PMIN-2(V) demonstrates much high TON of 121, greatly exceeding all the previous non-noble metal catalysts and comparable to the supported Ru nanoparticles (Table S3).

In summary, POM anions are successfully used as anionic building blocks for crosslinking cationic polyviologens into a series of novel mesoporous ionic networks with intrinsic catalytic functionalities. Large surface area and high density of active sites attains by using V-containing POM anions. The obtained hybrids perform as highly efficient and stable heterogeneous catalyst in aerobic oxidation of HMF to DFF with ambient O₂. This work described ionic self-assembly strategy provides an effective route to versatile porous POM solid materials, and more ionic cluster-based porous ionic networks would be rapidly emerged towards diverse applications.

The authors thank greatly the National Natural Science Foundation of China (Nos. 21136005, 21303084 and 21476109), Jiangsu Provincial Science Foundation for Youths (No. BK20130921), Specialized Research Fund for the Doctoral Program of Higher Education (No. 20133221120002).

Notes and references

View Article Online

DOI: 10.1039/C6DT00070C

- A. G. Slater and A. I. Cooper, *Science*, 2015, **348**, 8075.
- H. Furukawa, K. E. Cordova, M. O'Keeffe, O. M. Yaghi, *Science*, 2013, **341**, 1230444.
- S. Ding and W. Wang, *Chem. Soc. Rev.*, 2013, **42**, 548.
- Y. Zhang and S. N. Riduan, *Chem. Soc. Rev.*, 2012, **41**, 2083.
- Y. He, S. Xiang and B. Chen, *J. Am. Chem. Soc.*, 2011, **133**, 14570.
- P. Li, Y. He, Y. Zhao, L. Weng, H. Wang, R. Krishna, Hui Wu, W. Zhou, M. O'Keeffe, Y. Han and B. Chen, *Angew. Chem.*, 2015, **127**, 584.
- S. Fischer, J. Schmidt, P. Strauch and A. Thomas, *Angew. Chem. Int. Ed.*, 2013, **52**, 12174.
- Y. Yuan, F. Sun, L. Li, P. Cui and G. Zhu, *Nat. Commun.*, 2014, **5**, 4260.
- P. Zhang, Z. Qiao, X. Jiang, G. M. Veith and S. Dai, *Nano Lett.*, 2015, **15**, 823.
- G. Chen, Y. Zhou, X. Wang, J. Li, S. Xue, Y. Liu, Q. Wang and J. Wang, *Sci. Rep.*, 2015, **5**, 11236.
- X. Wang, Y. Zhou, Z. Guo, G. Chen, J. Li, Y. Shi, Y. Liu and J. Wang, *Chem. Sci.*, 2015, **6**, 6916.
- C. F. J. Faul and M. Antonietti, *Adv. Mater.*, 2003, **15**, 673.
- C. F. J. Faul, *Acc. Chem. Res.*, 2014, **47**, 3428.
- Y. Song and R. Tsunashima, *Chem. Soc. Rev.*, 2012, **41**, 7384.
- Y. Zhou, G. Chen, Z. Long and J. Wang, *RSC Adv.*, 2014, **4**, 42092.
- W. Qi and L. Wu, *Polym Int*, 2009, **58**, 1217.
- T. Lunkenbein, M. Kamperman, Z. Li, C. Bojer, M. Drechsler, S. Förster, U. Wiesner, A. H. E. Müller and J. Brey, *J. Am. Chem. Soc.*, 2012, **134**, 12685.
- J. E. Houston, A. R. Patterson, A. C. Jayasundera, W. Schmitt and R. C. Evans, *Chem. Commun.*, 2014, **50**, 5233.
- N. Liu, H. Wang and W. Bu, *J. Mater. Chem. C*, 2014, **2**, 5271.
- C. Tan, N. Liu, B. Yu, C. Zhang, W. Bu, X. Liu and Y. Song, *J. Mater. Chem. C*, 2015, **3**, 2450.
- A. Factor and G. E. Heinsohn, *J. Polym. Sci. B: Polym. Lett.*, 1971, **9**, 289.
- J. Sun and J. Zhang, *Dalton Trans.*, 2015, **44**, 19041.
- M. V. Vasylyev and R. Neumann, *J. Am. Chem. Soc.*, 2004, **126**, 884.
- G. Chen, Y. Zhou, P. Zhao, Z. Long and J. Wang, *ChemPlusChem*, 2013, **78**, 561.
- G. Chen, Y. Zhou, Z. Long, X. Wang, J. Li and J. Wang, *ACS Appl. Mater. Interfaces*, 2014, **6**, 4438.
- S. Uchida, S. Hikichi, T. Akatsuka, T. Tanaka, R. Kawamoto, A. Lesbani, Y. Nakagawa, K. Uehara and N. Mizuno, *Chem. Mater.*, 2007, **19**, 4694.
- A. C. Kalita, C. R. Marchal and R. Murugavel, *Dalton Trans.*, 2013, **42**, 9755.
- P. Zhao, Y. Leng and J. Wang, *Chem. Eng. J.*, 2012, **204-206**, 72.
- C. Gao, G. Chen, X. Wang, J. Li, Y. Zhou and J. Wang, *Chem. Commun.*, 2015, **51**, 4969.
- K. Inumaru, *Catal. Surv. Asia*, 2006, **10**, 151.
- R.-J. van Putten, J. C. van der Waal, E. de Jong, C. B. Rasrendra, H. J. Heeres and J. G. de Vries, *Chem. Rev.*, 2013, **113**, 1499.
- I. Sádaba, Y. Y. Gorbanev, S. Kegnaes, S. S. R. Putluru, R. W. Berg and A. Riisager, *ChemCatChem*, 2013, **5**, 284.
- J. Chen, Y. Guo, J. Chen, L. Song and L. Chen, *ChemCatChem*, 2014, **6**, 3174.
- F. Xu and Z. Zhang, *ChemCatChem*, 2015, **7**, 1470.
- A. Takagaki, M. Takahashi, S. Nishimura and K. Ebitani, *ACS Catal.*, 2011, **1**, 1562.
- Z. Zhang, Z. Yuan, D. Tang, Y. Ren, K. Lv and B. Liu, *ChemSusChem*, 2014, **7**, 3496.